



# Reinforcement of starch film with *Castanea sativa* shells polysaccharides: Optimized formulation and characterization

Leonardo Amaral<sup>a</sup>, Francisca Rodrigues<sup>a</sup>, Aurora Silva<sup>a,b</sup>, Paulo Costa<sup>c,d</sup>,  
Cristina Delerue-Matos<sup>a</sup>, Elsa F. Vieira<sup>a,\*</sup>

<sup>a</sup> REQUIMTE/LAQV, Polytechnic of Porto – School of Engineering, Rua Dr. António Bernardino de Almeida, 4249-015 Porto, Portugal

<sup>b</sup> Nutrition and Bromatology Group, Faculty of Food Science and Technology, Ourense Campus, Universidade de Vigo, E32004 Ourense, Spain

<sup>c</sup> UCIBIO – Applied Molecular Biosciences Unit, MedTech-Laboratory of Pharmaceutical Technology, Faculty of Pharmacy, University of Porto, 4050-313 Porto, Portugal

<sup>d</sup> Associate Laboratory i4HB – Institute for Health and Bioeconomy, Faculty of Pharmacy, University of Porto, 4050-313 Porto, Portugal

## ARTICLE INFO

### Keywords:

*Castanea sativa* shells

Polysaccharides

Starch-based film

Responsive surface methodology

## ABSTRACT

Chestnut (*Castanea sativa*) shells, generated from the peeling process of the fruit, contains appreciable amounts of lignin and cellulose. In this work, a starch-based film reinforced with these polysaccharides was developed. Response Surface Methodology was employed to optimize the composition of the film with improved elongation, tensile strength, and elasticity modulus properties. The optimal film was characterized regarding structural, optical barrier and thermal properties. The optimum composition was obtained with 10% (w/w) fibers and 50% (w/w) glycerol; the elongation responses, tensile strength and modulus of elasticity reached values of 34.19%, 7.31 N and 4.15 N, respectively. The values of tension strength and modulus of elasticity were approximately 3.5 times higher than those obtained for the control film. The reinforced film was opaque and exhibited improved water solubility, UV-barrier capacity, and thermal stability compared to control. The optimized starch film based on chestnut shells fibers' has the potential to produce biodegradable food packaging with improved properties.

## 1. Introduction

Biodegradable films have attracted increased attention from the food packaging industry because they can partly substitute or replace traditional non-biodegradable plastic films, which causes global pollution (Bangar et al., 2021; Matthews, Moran, & Jaiswal, 2021). According to PlasticsEurope, the environmental impact caused by synthetic packaging should be reduced by 55% until 2030 (European Commission, 2018). To establish this goal, numerous studies have been conducted to find promising biodegradable alternatives based on polysaccharides, lipids, and proteins materials (Hamed, Jakobsen, & Lerfall, 2021). Among polysaccharides, starch from different sources has been commonly used to develop biodegradable films due to their high availability and biodegradability, low cost, odorless, colorless, and nontoxic properties (Domene-López, Delgado-Marín, Martín-Gullon, García-Quesada, & Montalbán, 2019; Lisitsyn et al., 2021). However, its application to food packaging is limited due to the strong hydrophilicity, responsible for poor tensile strength and poor water barrier properties, as well as undesirable characteristics, namely brittle and

vulnerability to moisture (Bangar et al., 2021; Lisitsyn et al., 2021). The improvement of starch-based materials properties is, therefore, an ongoing challenge. One way to improve the mechanical properties is by producing composite films, which are created by incorporating compatible components into the starch polymeric matrix. Microcrystalline cellulose and carboxymethylcellulose have been commonly added to the starch-polymer matrix (Lisitsyn et al., 2021). These fillers have been reported to increase the tensile strength, elastic modulus, glass transition temperature, and water contact angle properties, and decrease the elongation, water vapor permeation, oxygen permeation, moisture, and water absorption properties of starch-based films (Dias, Müller, Larotonda, & Laurindo, 2011; Versino & García, 2014; Collazo-Bigliardi, Ortega-Toro, & Chiralt Boix, 2018; Harini, Mohan, Ramya, Karthikeyan, & Sukumar, 2018; Wu et al., 2019; Menzel, 2020). Likewise, fibers extracted from different food materials, namely cassava (Versino & García, 2014; Harini et al., 2018; Wu et al., 2019), coffee, rice, and sunflower husks (Collazo-Bigliardi et al., 2018; Menzel, 2020), apricot and walnut shells (Ali et al., 2019), sugarcane (Dos Santos, de Souza do Prado, Jacinto, & da Silva Spinacé, 2018) and eucalyptus (Dias

\* Corresponding author.

E-mail addresses: [elsavieiraf@gmail.com](mailto:elsavieiraf@gmail.com), [elsa.vieira@graq.isep.ipp.pt](mailto:elsa.vieira@graq.isep.ipp.pt) (E.F. Vieira).

<https://doi.org/10.1016/j.foodchem.2022.133609>

Received 16 February 2022; Received in revised form 3 June 2022; Accepted 28 June 2022

Available online 6 July 2022

0308-8146/© 2022 Elsevier Ltd. All rights reserved.

et al., 2011) have been pointed as suitable fillers to improve the mechanical properties of starch-based films. The addition of piassava lignin was also reported to increase the tensile strength and elastic modulus of starch-based film, although a decrease of elongation was observed (Souza de Miranda et al., 2015). Besides the positive impact on the mechanical properties, these fillers could improve some bio-functional properties of the reinforced films. For instance, literature reports that lignin, released in the produced lignin-based film, positively affects its antimicrobial and antioxidant properties (Mariana et al., 2021).

Portugal is one of the biggest European producers of chestnut (*Castanea sativa* Mill), being Trás-os-Montes region the most important production area, with 85% of the national production/total area of 35,000 ha/production of 19,000 tonnes per year (FAO, 2019). Chestnut shells (CS) represent approximately 20% of the fresh fruit weight and is generated from the peeling process of the chestnut fruit. This agronomic waste contains 36% (w/w) of polysaccharides, mostly represented by lignin (41.7%), cellulose (28.4%), and xylan (7.9%) (Morana et al., 2017). No previous studies have been reported on the formulation of starch-based films using fibers and lignin biopolymers extracted from CS. Thus, this research work aims to explore the potential of the polysaccharides extracted from this important Portuguese agro-food residue, to reinforce biodegradable starch-based films for packaging purposes. The formulation of the starch-based film reinforced with these biopolymers using different amounts of glycerol was first optimized via Response Surface Methodology (RSM). Then, the optimal formula was characterized regarding mechanical (elongation at break, tensile strength, elastic modulus, and thickness), optical (surface color, opacity, transparency), physical (humidity and water solubility), thermal (dynamic mechanical thermal analysis) and surface (scanning electron microscopy analysis) properties.

## 2. Material and methods

### 2.1. Material and chemicals

Potato starch, sodium chlorite, sodium azide, acetic acid, and glycerol ( $\geq 94\%$ ) were purchased from Sigma-Aldrich (Steinheim, Germany). Sodium hydroxide was obtained from LabKem (Barcelona, Spain) and sulfuric acid (96%) was purchased from Carlo Erba Reagents (Lisboa, Portugal). All the aqueous solutions were prepared with ultrapure deionized water ( $18.2 \text{ M}\Omega \text{ cm}^{-1}$  resistivity) from a Simplicity 185 water purification system (Millipore, Molsheim, France).

### 2.2. Chestnut shells (CS)

Chestnut shells (CS) were kindly supplied by Sortegel, located in Sortes (Bragança, Portugal), in October 2019. CS were dehydrated (Excalibur Food Dehydrator, USA) at  $42^\circ\text{C}$  for 24 h, grounded in a miller (Moulinex®) to particles sizes of 1 mm, and sieved in  $500 \mu\text{m}$  and  $100 \mu\text{m}$  mesh to separate the outer shell solids from the inner shell solids. Afterward, the inner shell solids were thoroughly mixed and stored at room temperature ( $20^\circ\text{C}$ ) under light-free conditions, until use.

### 2.3. Extraction of chestnut fiber (CF) and lignin (CL)

Chestnut fibers (CF) were extracted using the methodology described by Collazo-Bigliardi et al. (2018), with minor modifications. Sieved CS were alkali treated with 5% (w/v) and 10% (w/v) NaOH in 1:15, 1:20 and 1:30 solid:liquid (g/mL) ratios for 3 h at  $80^\circ\text{C}$ . This process was repeated 3 times. Then, the suspended CF were washed with pure water until the complete removal of the alkali solution. The black liquor was further used for the lignin extraction step. The bleaching treatment of CF was performed by adapting the Wu et al. (2019) protocol. Briefly, CF was added to 1:1 mixture of 5% (w/v)  $\text{NaClO}_2$  aqueous solution and acetic acid in a solid:liquid ratio of 1:20 g/mL, for 2 h, at  $80^\circ\text{C}$ . The bleached fibers were washed with pure water, dried for 24 h at  $42^\circ\text{C}$ ,

and milled. The chestnut lignin (CL) extraction was performed according to Souza de Miranda et al. (2015) procedure, wherein lignin is obtained by precipitation. For that, concentrated sulfuric acid was added to the black liquor obtained in the previous alkali treatment, the mixture was filtrated, and the solid lignin obtained was dried for 24 h at  $50^\circ\text{C}$ . Both CF and CL fractions were submitted to ultra-turrax (T10, Ika, Wilmigton, USA) to facilitate their dispersion on starch-films and stored at room temperature ( $20^\circ\text{C}$ ) under light-free conditions, until use.

### 2.4. Experimental design, modelling, and optimization

#### 2.4.1. Range of independent variables for Box-Behnken design (BBD) optimization

Preliminary studies were undertaken using a univariate method to make sure that possible maximum and minimum points of RSM were achieved. The glycerol concentration was evaluated between 10 and 80% w/w relative to starch (r.s.); showing that a concentration higher than 75% (w/w) produced films very sticky and hardly detached from mold. Oppositely, glycerol concentrations below 25% (w/w) resulted in a starch film extremely brittle. Considering these results, the content of glycerol was established between 40 and 60% (w/w) for the BBD experimental design. The CF concentration was evaluated between 5 and 18% (w/w); when CF was added in concentrations higher than 10% (w/w) it was inefficiently mixed with starch, making empty spots among fibers. In opposite, adding CF in concentrations below 10% (w/w), CF was entirely included in starch, not showing weaker or empty spots. Based on these results, the range of CF was settled between 0 and 10% (w/w) in the BBD optimization. CL was tested up to 66% (w/w). The results revealed that for a CL content  $>5\%$  (w/w) the starch film was too brittle to detach. Also, when the amount of CL was above 30% (w/w), the film easily cracks during the casting process. Thus, the composition of lignin to be tested was defined between 0 and 5% (w/w).

#### 2.4.2. Box-Behnken design (BBD)

Response surface methodology (RSM) was used to investigate the influence of the independent variables on the mechanical properties of starch-based film reinforced with CF and CL and to optimize them. For this purpose, and based on the results of the preliminary experiments, a Box-Behnken Design (BBD) with three factors ( $X_1$ ,  $X_2$ ,  $X_3$ ) at three equidistant levels ( $-1$ ,  $0$ ,  $+1$ ) was used to optimize the best composition of the starch-based film reinforced with CS polysaccharides. The independent variables under study were the concentrations of glycerol ( $X_1$ , at 40, 50 and 60% w/w r.s.), chestnut fiber ( $X_2$ , CF at 0, 5 and 10% w/w r.s.) and chestnut lignin ( $X_3$ , CL at 0, 2.5 and 5% w/w r.s.). The dependent variables under study included the following mechanical features: elongation at break ( $Y_1$ , %), tensile strength ( $Y_2$ , N), and elastic modulus ( $Y_3$ , N). The experimental design consisted of 17 combinations (Table 1) and each run was performed in triplicate. For the BBD analysis, two test pieces were randomly cut from each film, avoiding bubbles and other fragilizing structures. The optimal values of responses  $Y$  were obtained by solving the regression equations and by analysing the responses surface and contour plots using the predictive equations of RSM. A set of experiments using the critical values optimized was conducted to test the accuracy of the model.

### 2.5. Films preparation

Films were produced according to Souza de Miranda et al. (2015) protocol. The quantity of starch was fixed to 2.5 wt% and the amounts of glycerol, CL and CF were variable according to the experimental design (Table 1). The film composition was mixed in water at  $80^\circ\text{C}$  for 30 min with continuous mechanical stirring. Then, 40 mL of the mixture were transferred to a silicone mold and dried on an oven (JP Selecta, Model 20002) at  $50^\circ\text{C}$  for 12 h. After detaching, films were conserved in a desiccator for further analysis.

**Table 1**

Experimental design for evaluation of the effects of glycerol (X1, % w/w r.s.), chestnut shells fibers, CF (X2, % w/w r.s.) and chestnut shells lignin, CL (X3, % w/w r.s.) on elongation at break (Y1, %) tensile strength (Y2, N) and elastic modulus (Y3, N) of starch-based films.

Point <sup>a</sup>	Independent variables			Dependent variables						
	run	X1Glycerol, % w/w r.s.	X2CF, % w/w r.s.	X3CL, % w/w r.s.	Y1, Elongation at break (%)		Y2, Tensile strength (N)		Y3, Elastic modulus (N)	
					Exp <sup>b</sup>	Pred <sup>c</sup>	Exp <sup>b</sup>	Pred <sup>c</sup>	Exp <sup>b</sup>	Pred <sup>c</sup>
1	40	0	2.5		35.45 ± 4.48	36.08	1.50 ± 0.14	1.52	0.98 ± 0.16	0.99
2	50	5	2.5		18.33 ± 1.11	20.11	3.18 ± 0.29	2.85	1.88 ± 0.28	1.73
3	50	5	2.5		17.68 ± 2.08	20.11	3.43 ± 0.33	2.85	1.99 ± 0.20	1.73
4	60	10	2.5		22.59 ± 1.01	21.96	5.48 ± 1.12	5.46	3.46 ± 0.91	3.45
5	50	0	5		46.07 ± 13.4	46.10	3.60 ± 0.74	3.96	2.51 ± 0.15	2.76
6	60	0	2.5		51.50 ± 5.78	47.49	2.64 ± 0.09	1.38	1.31 ± 0.09	0.57
7	40	5	5		20.79 ± 4.14	20.13	4.14 ± 0.38	3.76	3.43 ± 0.28	3.17
8	40	5	0		26.67 ± 3.37	22.69	3.17 ± 0.44	2.28	1.73 ± 0.17	1.24
9	50	5	2.5		20.55 ± 1.73	20.11	2.72 ± 0.33	2.85	2.06 ± 0.03	1.73
10	50	0	0		36.67 ± 3.27	40.02	1.44 ± 0.04	2.32	0.71 ± 0.05	1.19
11	60	5	0		26.95 ± 3.00	27.61	2.42 ± 0.26	2.80	1.25 ± 0.16	1.51
12	50	5	2.5		25.60 ± 2.50	20.11	3.10 ± 0.91	2.85	1.24 ± 0.16	1.73
13	50	5	2.5		18.38 ± 2.33	20.11	1.81 ± 0.19	2.85	1.50 ± 0.17	1.73
14	40	10	2.5		24.04 ± 1.21	28.05	4.45 ± 0.51	5.70	2.89 ± 0.54	3.63
15	50	10	5		21.79 ± 3.30	18.43	8.11 ± 0.86	7.23	5.80 ± 0.25	5.32
16	50	10	0		34.17 ± 11.5	34.14	7.67 ± 0.63	7.31	4.40 ± 0.42	4.16
17	60	5	5		16.56 ± 0.99	20.54	1.97 ± 0.10	2.87	1.80 ± 0.16	2.30

<sup>a</sup> Experiments were performed in a random order.

<sup>b</sup> Results are expressed as mean ± standard deviation (n = 3).

<sup>c</sup> Based on BBD evaluation. CF, chestnut shells fibers; CL, chestnut shells lignin.

## 2.6. Films characterization

Films were kept in desiccators containing silica gel at room temperature (25 ± 3 °C) during analysis of mechanical (elongation at break, tensile strength, elastic modulus, and thickness), optical (surface color, UV-barrier capacity, opacity, transparency), physical (humidity and water solubility), thermal (dynamic mechanical thermal analysis) and surface (scanning electron microscopy analysis) properties.

### 2.6.1. Mechanical properties

The tensile properties (elongation at break, tensile strength, and elastic modulus) were evaluated using a texture analyser (Stable Micro Systems TA-XT2I, Goldalming, UK); the probe selected was the Miniature Tensile Grips for Tension analysis. Test speed was set to 0.10 mm/sec with trigger force of 0.049 N and a test distance of 100.00 mm. The equipment was previously calibrated for distance and force. The measure units for force, distance, and time were Newtons (N), millimeters (mm) and seconds (s), respectively. The test piece dimension of films for analysis was 30.0 × 10.0 mm. Results were collected using the Exponent Stable Micro Systems software (version 6.1.12.0). The test pieces thickness was measured with an Electronic Micrometer (0.001 mm).

### 2.6.2. Optical properties

Film colour was measured using an Avaspec-2048-TEC spectrometer (Avantes, Netherlands), calibrated with a standard (L\* = 99.87, a\* = -6.07, b\* = 12.24). The CIELab colour scale was used to determine a\*, b\* and L\* parameters, where a\* is the greenness and redness of samples, b\* represents the blueness and yellowness, and L\* is the luminosity. Colour assays were performed by placing the film samples over the white plate. Samples were analysed in triplicate, recording five measurements at different positions for each sample. The coordinates for a\* and b\* were used to calculate h° (hue angle) (Eq. (1)), corresponding to the colour itself, and C\* or chroma, corresponding to the intensity of the colour (Eq. (2)).

$$h^{\circ} = \tan^{-1} \left( \frac{b^*}{a^*} \right) \quad (1)$$

$$C^* = \sqrt{(a^*)^2 + (b^*)^2} \quad (2)$$

For the evaluation of UV-barrier capacity, film samples were cut with

scissors into bars of 10 × 30 mm and placed into a quartz cell. The absorbance spectrum between 200 and 700 nm was registered using a Shimadzu UV-2101PC (Kyoto, Japan) spectrophotometer, with an empty test cell as reference. The area under the curve between 200 and 400 nm, expressed as absorbance units per nanometer (AU × nm), estimated the UV-barrier capacity of films, while the area under the curve between 400 and 700 nm determined the film opacity. Film transparency was calculated as the absorbance value at 600 nm divided by film thickness and was expressed as A600/mm.

### 2.6.3. Humidity and water solubility

Humidity content (%) was determined by measuring the weight loss of films, upon drying in an oven at 105 °C until constant weight. The water solubility of the films was determined, in triplicate, as described by Silva et al. (2020). Films were cut with a scalpel in an approximately circular format (~20 mm diameter) and three disks of each film were dehydrated in the ventilated oven at 105 °C for 24 h. After 30 min in a desiccator with silica gel, each sample was weighed (initial dry weight, Wi) and transferred to a beaker with 50 mL of distilled water containing sodium azide (0.02% w/v) and kept at room temperature (25 ± 3 °C) for 24 h with occasional agitation. The water was drained, and the samples were dried at 105 °C for 24 h. The resulting material was weighed to determine the final dry weight (Wf), and the percentage of water solubility (S) was determined using Eq. (3).

$$S(\%) = \frac{W_i - W_f}{W_i} \times 100 \quad (3)$$

### 2.6.4. Thermal properties

The analysis of thermal stability of film samples was performed by a NETZSCH TG 209F3 (Gebrüder-Netzsch-Straße, Germany) thermogravimetric analyser and analyzed by a Proteus VSM (Virtual System Modeling) software. Samples (3.0–5.0 mg) were placed in aluminum crucibles inside the thermogravimetric balance and then heated under nitrogen atmosphere (60 mL min<sup>-1</sup>) in the range of 30 to 550 °C at a heating rate of 10 °C min<sup>-1</sup>.

### 2.6.5. Morphology characterization

Scanning electron microscopy (SEM) was used to observe the surface morphology and the cross-sections of reinforced starch-based films. The film samples were cut with a scalpel and fixed on support stubs,

previously covered with carbon tape and gold coated, for the evaluation of surface morphology and cross-section using SEM (FEI Quanta 400FEG ESEM/EDAX Genesis X4M) equipment.

## 2.7. Statistical analysis

Results were presented as mean  $\pm$  standard deviation. The Design Expert trial version 7 (Stat-Ease Inc., Minneapolis, MN, USA) was used for the analysis of the response surface and contour plots and the statistical analysis of the BBD model. Analysis of variance (ANOVA) was performed, and regression coefficients of linear, quadratic, and interaction terms were determined. Adequacy of the model was evaluated using model analysis, coefficient of determination ( $R^2$ ), and lack-of-fit test. Significance of the equation was determined by  $F$  value at a probability ( $p > F$ )  $< 0.05$ . The  $t$ -test was conducted to compare the responses prepared under optimized conditions with those predicted by BBD model.

## 3. Results and discussion

### 3.1. Alkali treatment

Two different concentrations of NaOH solutions (5 and 10 % w/v) at three solid:liquid ratios (1:15, 1:20 and 1:30 g/mL) were tested for the CF alkali extraction. Fig. A.1 shows the visual differences of CF obtained under different alkali treatment conditions. Results from Fig A.1. (A)(C) versus (D)(E) suggest no differences between 5 % (w/v) and 10 % (w/v) NaOH solution treatments. However, as observed in Fig A.1. (C) and (E), a cleaner CF was obtained using a 1:30 solid:liquid ratio (g/mL) treatment. Based on these results, the best conditions for the alkali treatment of CF were 5 % (w/v) NaOH solution and a 1:30 solid:liquid ratio (g/mL). Applying this cleaning condition, the residue yield of CF was  $26.1 \pm 1.2$  % and the reagents consumption was minimized. Excluding the subsequent extraction step of lignin, and in a perspective of a sustainable laboratorial practice, we tested the reuse of the alkali solution to extract CF from new milled chestnut shell material. This procedure was however inefficient, promoting  $7.1 \pm 0.8$  % residue yield of CF.

### 3.2. Validation of the experimental design

The experimental conditions and the experimental and predicted values of the responses elongation (Y1), tensile strength (Y2) and elastic modulus (Y3), used to optimize the starch-based film reinforced with polysaccharides from chestnut shells, are shown in Table 1. As observed, the three responses were in accordance with the predicted values. The experimental Y1, Y2 and Y3 values for the control film (run 10: 50 % w/w r.s. glycerol and 0% of CF and CL) were respectively  $36.67 \pm 3.27\%$ ,  $1.44 \pm 0.04$  N and  $0.71 \pm 0.05$  N. The elongation (Y1) ranged between 16.56 % (run 17) and 51.50 % (run 6); the tensile strength varied from 1.44 (run 10) to 8.11 N (run 15), and the elastic modulus ranged between 0.71 (run 10) and 5.80 N (run 15). Overall, the addition of CF conducted to starch-based films with the worst elongation, but higher tensile strength and elastic modulus mechanical properties compared to control film. For instance, under the experimental conditions of run 16 (CF = 10 % w/w r.s. and CL = 0% w/w r.s.), the developed starch-based films presented an elongation value of  $34.17 \pm 11.5\%$  and respective tensile strength and elastic modulus values of  $7.67 \pm 0.63$  N and  $4.40 \pm 0.42$  N. In contrast, starch-based films without CF (runs 5 and 6) presented higher elongation compared to the control film, the respective values obtained were  $46.07 \pm 13.4$  and  $51.50 \pm 5.78$ . Results also suggested that the combined addition of CF and CL (run 15: CF = 10 % w/w r.s. and CL = 5% w/w r.s.) resulted in starch-based film with worst elongation ( $21.79\% \pm 3.30$ ) but better tensile strength ( $8.11 \pm 0.86$  N) and elastic modulus ( $5.80 \pm 0.25$  N) properties compared to the control film.

The model summary and the results obtained from the ANOVA

analysis of the BBD in the response surface quadratic model are shown in Table A.1. The independent variable X1 (% w/w r.s. glycerol) had no significant effect on any response ( $p > 0.05$ ), while the independent variable X2 (% w/w r.s. CF) showed a significant effect on the three responses ( $p < 0.01$ ). The independent variable X3 (% w/w r.s. CL) only exhibited a significant effect on elastic modulus ( $p = 0.0187$ ). The quadratic term for X1 showed no significant effect on any response, while the quadratic term for X2 was significant for elongation ( $p = 0.0005$ ), tensile strength ( $p = 0.0283$ ) and elastic modulus ( $p = 0.0266$ ) responses. The quadratic term of X3 only showed significance on elastic modulus ( $p = 0.0437$ ). The coefficient of determination ( $R^2$ ) is an indicator of the proximation of real points to the prediction model. This value may range from 0 to 1; closer to 1 means a better fit of data on the model (Prabha & Ranganathan, 2018). According to  $R^2$  adjust values, the quadratic models explained, respectively, 82.05, 87.82 and 77.63% of the variation of glycerol, CF, and CL composition on elongation (Y1), tensile strength (Y2) and elastic modulus (Y3) properties of starch-based film. The “lack of fit” for the three responses was not significant ( $p > 0.05$ ) and the Ratio was higher than 4 (as desirable), indicating an appropriate signal-to-noise ratio and good adequacy of the model to predict Y1, Y2 and Y3 responses. The quadratic polynomial model for the three responses was regressed and expressed in terms of coded factors as follows:

$$\begin{aligned} \text{Elongation (\%)} = & 20.11 + 1.33X_1 - 8.39X_2 - 2.41X_3 - 4.38X_1.X_2 - \\ & 1.13X_1.X_3 - 5.45X_2.X_3 + 0.68X_{12} + 12.61X_{22} + 1.96X_{32} \end{aligned} \quad (4)$$

$$\begin{aligned} \text{Tensile Strength (N)} = & 2.85 - 0.09X_1 + 2.07X_2 - 0.39X_3 - 0.03X_1.X_2 \\ & - 0.35X_1.X_3 - 0.43X_2.X_3 - 0.81X_{12} + 1.47X_{22} \\ & + 0.89X_{32} \end{aligned} \quad (5)$$

$$\begin{aligned} \text{Elastic Modulus (N)} = & 1.73 - 0.15X_1 + 1.38X_2 + 0.68X_3 + 0.06X_1.X_2 \\ & - 0.29X_1.X_3 - 0.10X_2.X_3 - 0.44X_{12} + 0.86X_{22} \\ & + 0.76X_{32} \end{aligned} \quad (6)$$

Model equations are visualized in the form 3D surface plots, which are constructed by plotting the response on the Z-axis against any two independent variables while maintaining other variables at their optimal levels. Fig. 1 displays nine different 3D surface plots: (A), (B) and (C) are related to elongation response; (D), (E) and (F) are associated with tensile strength while (G), (H) and (I) are associated to the elastic modulus. Fig. 1 (A-C) suggests that higher elongation could be promoted with 60 % w/w r.s. of glycerol and 5.0% w/w r.s. of CL. Glycerol acts as plasticizer, allowing the film to be more elastic, while the addition of fillers compromises elongation, making the starch film stiffer. The 3D surface plots of tensile strength and elastic modulus have identical shape when correlating the same independent variables. In 3D surface plots (D) and (G), the highest point is observed using the highest amount of CF (10 % w/w r.s.) and 50 % w/w r.s. of glycerol. According to 3D surface plots (E) and (H), higher values of elastic modulus are achieved using glycerol at 45–50 % w/w r.s.

### 3.3. Experimental design, response surface method and validation

The performance of BBD model in predicting the optimum composition of starch-based film reinforced with CS polysaccharides was evaluated. Desirability indices were constructed to obtain the optimum experimental conditions to maximize the three mechanical properties of reinforced starch-based film, and confirmatory experiments were performed to compare the experimental results with those predicted by the model. The optimal composition to maximize the elongation of the reinforced starch-based film was 60 % w/w r.s. of glycerol and 5% w/w

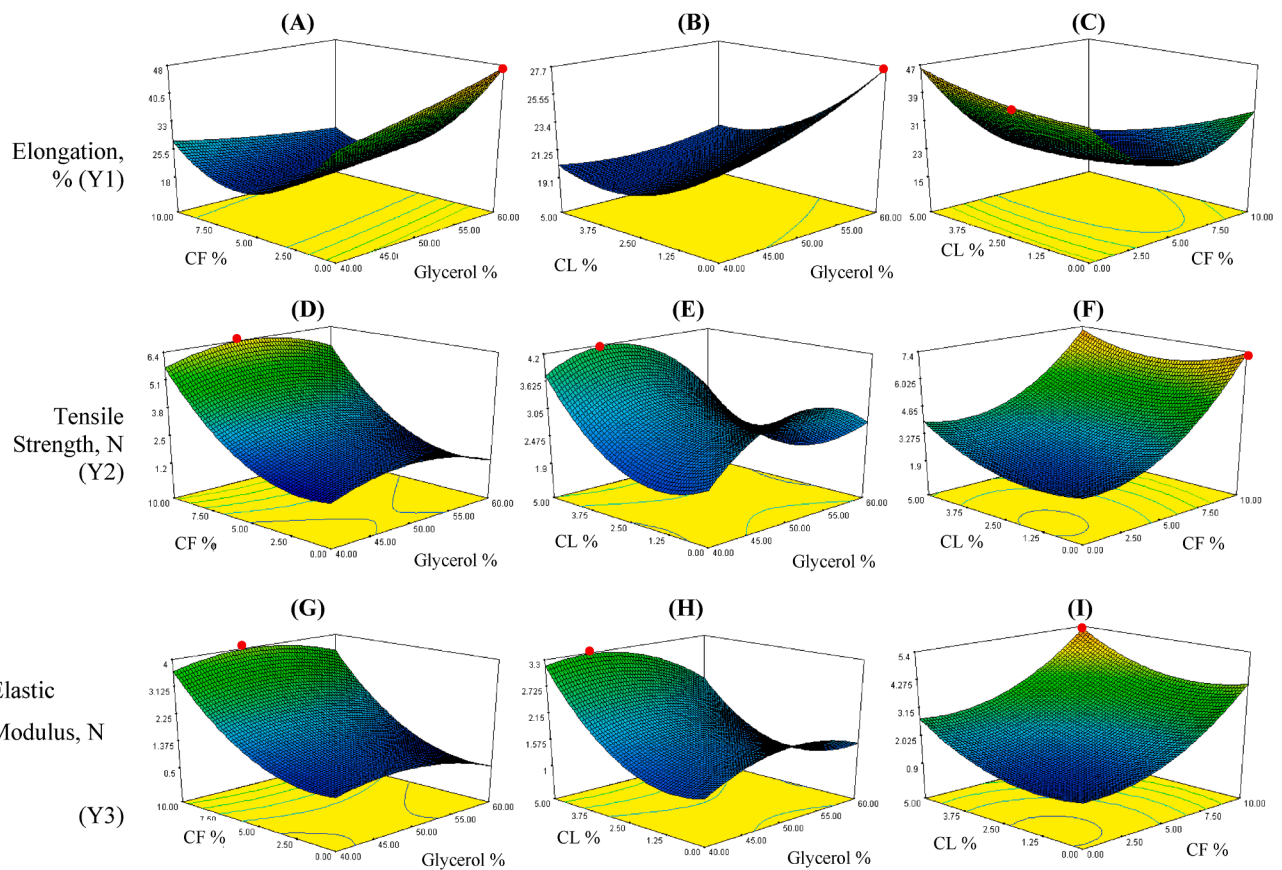


Fig. 1. Response surface 3D plots for BBD correlating independent variables to the three responses: Y1 - Elongation [(A), (B) and (C)], Y2 - Tensile Strength [(D), (E) and (F)] and Y3 - Elastic Modulus [(G), (H) and (I)], while maintaining the third independent variable at its middle level.

Table 2

Tensile properties comparison of starch-based films obtained on present work with starch-based films reported in literature.

Starch	Glycerol (w/w r.s.)	Reinforcement (w/w r. s.)	Code	Method	Elongation (%)	TensileStrength	ElasticModulus	Reference
2.5% wt. Potato	50%	0% CF + 0% CL (run 10) *	A1	Casting	36.67 ± 3.27	1.44 ± 0.04 N (1.26 ± 0.08 MPa)	0.71 ± 0.05 N (5.97 ± 0.58 MPa)	Present work
	50%	0% CF + 5% CL (run 5) *	A2		46.07 ± 13.4	3.60 ± 0.74 N (2.07 ± 0.39 MPa)	2.51 ± 0.15 N (7.45 ± 0.18 MPa)	
	50%	10% CF + 0% CL **	A3		34.17 ± 11.5	7.67 ± 0.63 N (5.55 ± 0.67 MPa)	4.40 ± 0.42 N (13.88 ± 0.66 MPa)	
5% wt. Corn	50%	–	B1	Casting	47.278 ± 2.994	1.717 ± 0.087 MPa	12.100 ± 0.944 MPa	(Souza de Miranda et al., 2015)
	10%	40% lignin	B2		3.239 ± 0.293	14.293 ± 1.883 MPa	673.500 ± 53.203 MPa	
5% wt. Cassava	50%	–	C1	Casting	50.697 ± 4.421	2.144 ± 0.193 MPa	21.600 ± 4.519 MPa	
	10%	40% lignin	C2		9.865 ± 2.844	20.153 ± 1.854 MPa	930.100 ± 96.479 MPa	
Corn	30%	50% water	D1	Extrusion	12 ± 7	13.0 ± 1.5 MPa	260 ± 80 MPa	(Collazo-Bigliardi, Ortega-Toro, & Chiralt Boix, 2018)
	30%	50% water + 10% coffee bleach fibers	D2		3 ± 1	19.0 ± 1.0 MPa	822 ± 38 MPa	
	30%	50% water + 10% rice bleach fibers	D3		3 ± 1	17.0 ± 3.0 MPa	863 ± 2 MPa	
5% wt. Corn	20%	0% cellulose nanofibers	E1	Casting	–	3.0 MPa	150 MPa	(Cheng, Zhou, Wei, Cheng, & Zhu, 2019)
	20%	10% microfibrillated cellulose	E2		–	9.5 MPa	650 MPa	

\* Experimental values obtained in the BBD (Table 1); \*\* Experimental values obtained for the optimized starch-based film reinforced with 10% w/w r.s of CF, chestnut shells fibers; CL, chestnut shells lignin. Tensile strength and elastic modulus values (MPa) were calculated according to Gonçalves et al., 2020.

r.s. of CL, with a desirability of 99.6 %. The tensile strength of the reinforced starch-based film was maximized using 51 % w/w r.s. of glycerol and 10% w/w r.s. of CF (desirability of 88.2 %) and the optimal composition to maximize the elastic modulus of the reinforced starch-based film was 46 % w/w r.s. of glycerol, 10% w/w r.s. of CF and 5% w/w r.s. of CL (desirability of 92.1%). For the three responses, the experimental conditions agreed (within a 95% confidence interval) with the predicted values (Table A.2) Individual desirability's were combined into a single number and then searched the greatest overall desirability. With a desirability of 76.9 %, the use of 50 % w/w r.s. of glycerol and 10% w/w r.s. of CF in the starch-based film formulation enable

elongation of 34.19%, a tensile strength of 7.31 N and an elastic modulus of 4.15 N. The experimental values for the three responses were in accordance with the predicted values by the model (within a 95% confidence interval), showing the effectiveness of the BBD for the optimization of the mechanical properties of the starch-based film reinforced with chestnut shell fibers (Table A.2). Under these experimental conditions, the values of tensile strength and elastic modulus were approximately 3.5 times higher than those obtained for the control film.

The starch-based films reinforced with CS polysaccharides developed in the present work were compared with those reported in the literature. In the present work, the use of CF to reinforce the potato starch-based

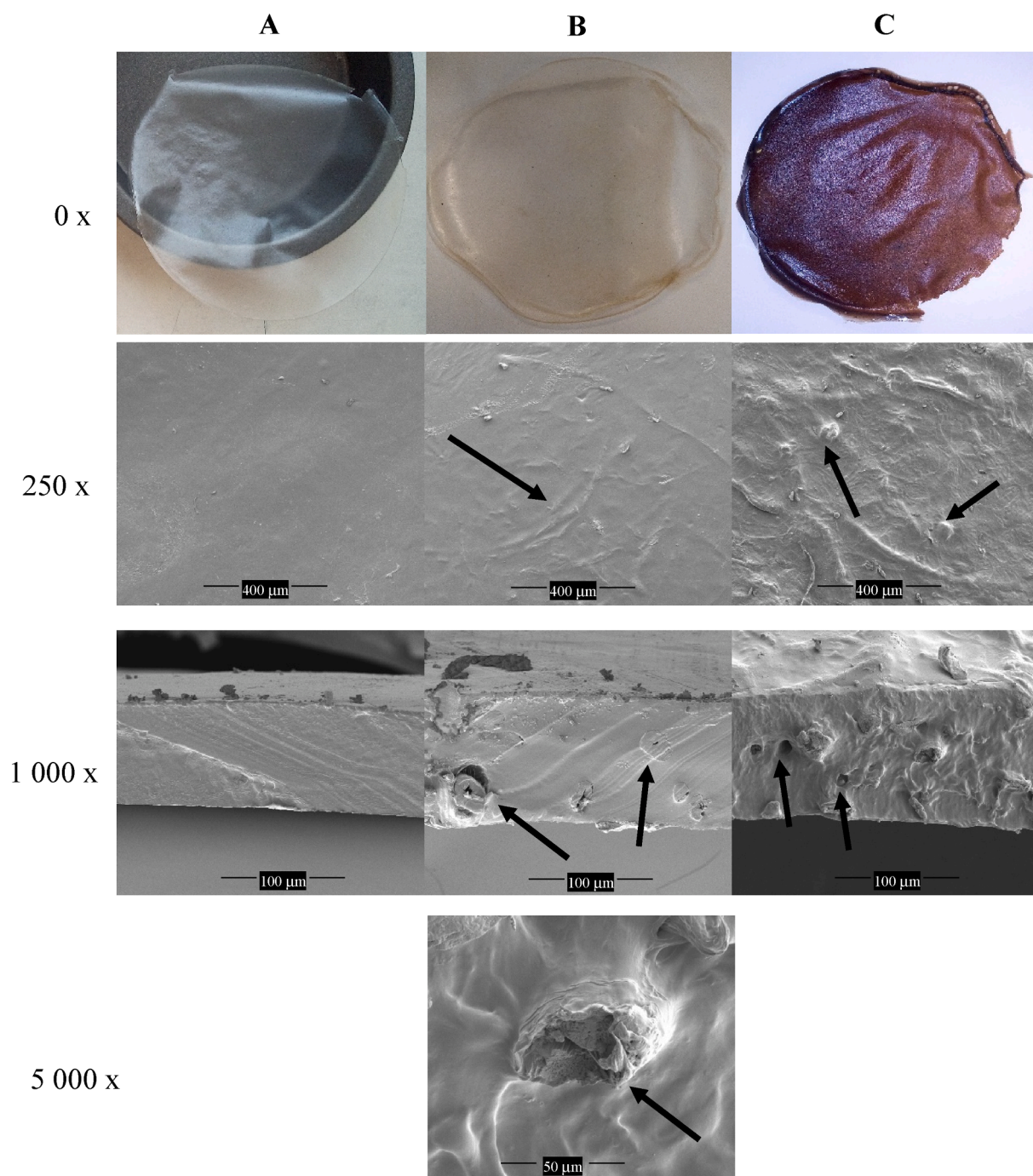


**Fig. 2.** Photographs (0 x) and SEM micrographs of surface (250 x) and cross-section (1 000× and 5 000 x) of starch-based films plasticized with 50% w/w r.s glycerol: (A) control film; (B) reinforced with 10% w/w r.s of CF (optimized formula); and (C) reinforced with 10% w/w r.s. of CF and 5% w/w r.s. of CL (run 15, Table 1). Legend: the black arrows indicate the CF and the CL components incorporated in the starch matrix.

film promoted an elongation maintenance, while tensile strength and elastic modulus increased 440% and 619%, respectively, for MPa units (A1, A3, Table 2). Collazo-Bigliardi et al. (2018) employed the extrusion method to produce corn starch-based films reinforced with 10% w/w r.s. of bleach fibers from coffee/rice sources. According to these authors, the addition of 10% w/w r.s. bleach fiber promoted a decrease by 7% of the initial value of the elongation but improved the tensile strength and the elastic modulus of films (D1, D2 (146% and 316%) and D1, D3 (130% and 331%). This smaller increase in tensile strength can be explained by differences on the used starch and on the methodology applied. These authors used corn starch and bleach fibers, and films were prepared by extrusion, while in the present work, potato starch was used, and films were produced by a casting process. Cheng, Zhou, Wei, Cheng, & Zhu (2019) also showed an increase of tensile properties (E1, E2, Table 2) closely to the ones reported in the present work (Indeed, an increase of 316% and 433% for tensile strength and elastic modulus, respectively, could be observed. Elongation was not evaluated, and the fillers used to reinforce the corn starch-based films were cellulose nanofibers and microfibrillated cellulose. The extraction of lignin from CS and the formulation of the reinforced film were according to Souza de Miranda et al. (2015) protocol. These authors varied the concentration of lignin and glycerol by a total of 50% w/w r.s., and piassava was the source of lignin. In the present work, it was not possible to obtain films with such composition, the incorporation of >5% w/w r.s. of CL made films brittle and easily crack during casting. Although the extraction methodology of lignin was similar, it is well known that different sources affect the composition and structures of lignin (Grossman & Vermerris, 2019). The preliminary results of this work showed a huge difference in the possible lignin composition of films. For this reason, it is possible that CL has different interactions with starch, making a more brittle and hardener film. Further studies of CL characterization may provide information regarding this topic. Concerning the tensile properties, Souza de Miranda et al. (2015) reported that reducing glycerol to 10% w/w r.s. and with the addition of 40% w/w r.s. of lignin decreased the elongation to 7% and 19% of initial value (B2 and C2, Table 2) for both corn- and cassava starch-based films. However, values of the tensile strength and elastic modulus increased 832% and 5566% for corn starch and 940% and 4306% for cassava starch. In the present work, the addition of CL up to 5% w/w r.s. to the potato starch-based films provided a small increase of tensile strength and elastic modulus, 164%, 125%, respectively, but a smaller increase of elongation, 126% (E1, E2, Table 2).

### 3.4. Scanning electron microscopy (SEM)

The morphological structure of the surface and the cross-section of the starch-based films reinforced with CF and CL developed in this work are shown in Fig. 2. The control film (A) is translucent and clear, the starch-based film reinforced with 10% w/w r.s. of CF (film B) is more yellow and less translucent, while the starch-based film reinforced with 10% w/w r.s. of CF and 5% w/w r.s. of CL (film C) has a brown colour and an opaquer appearance. From SEM analysis it is observed that the surface of control film (A) is clear and smooth (zoom 250 x), also presenting a cut clean (at a magnification of 1 000 x) without any visible deformation. The CF components of film B are visible on the surface and the cuts (pointed with black arrows at different zoom values). Micrographs of the film's surfaces at a magnification of 5 000× show the transactional cut of CFs and their adhesion to starch. It can be observed that the CFs are well cemented in the continuous phase, thus the homogeneous matrix of these films is a good indicator of their structural integrity. In the film (C), some CLs components are visible on the surface (pointed with black arrows at different zoom values), meaning that not all the lignin was dissolved in starch, creating some weaker spots.

**Table 3**

Properties of the optimized starch-based film reinforced with CF.

Property	Control film (50% w/w r.s. glycerol)	Optimized film (50% w/w r.s. glycerol and 10% w/w r.s. CF)
Thickness ( $\mu\text{m}$ )	114.22 $\pm$ 6.58	148.70 $\pm$ 30.01
Luminosity (L*)	97.94 $\pm$ 1.04	63.03 $\pm$ 1.65 *
Chroma (C*)	28.62 $\pm$ 1.63	26.36 $\pm$ 0.52 *
Hue angle (h°)	101.43 $\pm$ 3.11	94.90 $\pm$ 1.68
UV-barrier capacity (AU $\times$ nm)	129.36 $\pm$ 3.63	266.87 $\pm$ 2.65 *
Opacity (AU $\times$ nm)	138.63 $\pm$ 2.06	229.01 $\pm$ 2.32 *
Transparency (A600/ mm)	3.97 $\pm$ 0.47	4.92 $\pm$ 0.94
Humidity (%)	12.08 $\pm$ 1.07	20.09 $\pm$ 1.58 *
Water solubility (%)	42.88 $\pm$ 4.23	52.48 $\pm$ 3.96 *
T <sub>d</sub> (95%) (°C)	105.2	175.2 *
T <sub>max</sub> (°C)	275.0	315.8 *

Results are expressed as mean  $\pm$  standard deviation (n = 3).

TGA results evaluated at 5 wt% of weight loss (T<sub>d</sub> (95%)) and at temperatures of maximum degradation rate (T<sub>max</sub>).

\* Statistical difference at  $p \leq 0.05$  (Student's t-test).

CF, chestnut shells fibers; CL, chestnut shells lignin.

### 3.5. Characterization of the optimized starch-based film reinforced with CF

The optimized starch-based film was prepared with 50% w/w r.s. glycerol and 10% w/w r.s. CF was characterized regarding thickness, colour, UV-barrier capacity, opacity, transparency, humidity, water solubility, and thermal properties. Results are resented in Table 3.

Thickness is an important parameter since it may affect other properties, such as permeability and optical properties (Lisitsyn et al., 2021). The incorporation of CF did not affect the thickness of the starch film ( $p < 0.05$ ), the reinforced film presented a thickness of 148.70  $\pm$  30.01  $\mu\text{m}$ . Water solubility is another important parameter for the applicability of the film for packaging of foods with high water activity; materials with low water solubility are desirable to enhance the integrity of the food product and the water resistance (Silva et al., 2020). Solubility studies indicated that reinforced film with CF was water soluble and the incorporation of the filler into the starch matrix increased the solubility by 10% ( $p < 0.05$ ), suggesting a greater interaction of CF with the water. This result is correlated with the improved mechanical properties of the optimized film. Likewise, the addition of CF to the starch film resulted in higher moisture content, (around 8%,  $p < 0.05$ ) compared to the control film. The humidity of the optimized film was 12.08  $\pm$  1.07%. Both properties agree with other developed biodegradable films reported in the literature (Silva et al., 2020) but suggest the limited use of the optimized film in foods with high water content.

The optical properties of control and reinforced films are shown in Table 3. Luminosity (L) and Chroma (C\*) parameters decreased with the CF addition, while the change in hue angle (h°) remained constant. These results agree with the visual observations. Furthermore, it should be noticed that the decrease in luminosity parameter with filler addition agrees with the opacity increase. The incorporation of CF did not affect the transparency of the starch film. The study of the UV light absorption capacity of the optimized film is relevant to determine their possible applications for packaging. Fig. A.2 shows the obtained UV-Vis light absorption spectrum of starch-based films. Reinforced films UV spectra showed a characteristic peak at 250–300 nm, which could be mainly attributed to the phenolic components of chestnut shells (Pinto et al., 2021). To estimate the UV-barrier capacity of reinforced films, the area under the curve in the UV region was calculated. As it can be expected, this parameter significantly ( $p < 0.05$ ) increased with CF addition, the obtained value was 266.87  $\pm$  2.65 AU  $\times$  nm. A similar trend was observed for opacity in the visible region, the obtained value was 229.01  $\pm$  2.32 AU  $\times$  nm. Darker and opaque films can increase the protection

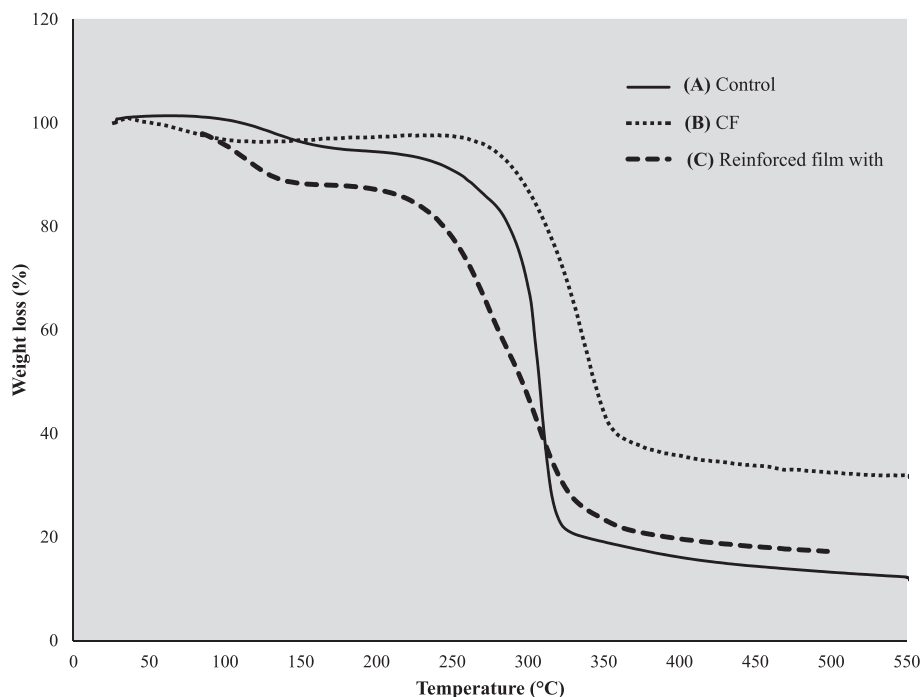


Fig. 3. TGA curves of (A) control film, i.e., without CF; (B) CF; and (C) starch-based film reinforced with 10% w/w r.s. of CF.

against the photo-oxidation of food (Silva et al., 2020). Thus, the colour of the starch-based film reinforced with CF can provide greater protection against light and UV radiation.

The thermal stability of starch film (control) and starch film reinforced with CF were evaluated by TGA. The TGA curves are shown in Fig. 3. CF (curve B) exhibited high thermal stability, maintaining their mass almost unaltered up to 250 °C (weight retention > 97%). The mass loss events between 250 and 350 °C could be attributed to the decomposition of bioactive constituents, mainly phenolic compounds (Pinto et al., 2021). The thermal degradation of control film (curve C) followed the typical pattern of glycerol-plasticized starch films described in the literature (García, Famá, Dufresne, Aranguren, & Goyanes, 2009; Piñeros-Hernandez, Medina-Jaramillo, López-Córdoba, & Goyanes, 2017). A small step of weight loss (c.a. 4%) between 30 and 150 °C could be attributed to water loss; the mass loss event between 150 and 200 °C could be attributed to the decomposition of the glycerol-rich phase (boiling point of glycerol is 198 °C); and at temperatures higher than 200 °C could occur the oxidation of the partially decomposed starch. In the reinforced starch film with CF (curve A), the degradation temperatures showed a shift towards higher values compared to the control film, suggesting a higher thermal stability. The temperatures corresponding to a weight loss of 5 wt% [ $T_{d(95\%)}$ ] and to the maximum degradation rate ( $T_{max}$ ) are summarized in Table 3. From the results, it can be found that control film shows a broad degradation step with an onset temperature of 105.2 °C (evaluated at 5 wt% of weight loss) and with a maximum degradation temperature of 175.2 °C under nitrogen flow. The incorporation of CF into starch matrix causes a shift of the onset degradation temperature toward higher temperature (about 70 °C ahead). This result suggests a good adhesion between the CF and the starch matrix, which reduces the mass loss in the reinforced film. In other words, the onset degradation temperature of starch can be significantly improved by the addition of the reinforced filler. This result is in line with other works, reporting that fiber addition to a starch matrix improves its thermal stability (Lomelí-Ramírez et al., 2014; Wu et al., 2019; Cheng et al., 2019).

#### 4. Conclusions

This work evaluated the effect of lignin and fibers extracted from

chestnut shells as reinforcement materials of starch-based films. Applying a Box-Behnken design model, the optimum composition of potato starch film incorporating these biopolymers with higher elongation, tensile strength, and elastic modulus properties was: 50% w/w r. s. glycerol and 10% w/w r.s. of CF. SEM micrographs evidenced that the CF was structurally incorporated in the starch matrix, the reinforced starch-based film was homogeneous with smooth microstructures, indicating good compatibility. Besides the improvement of the tensile properties, comparable to ones obtained by other authors, the CF addition increased film opacity while decreased luminosity parameter. Likewise, the reinforced film exhibited improved water solubility, UV-barrier capacity, and thermal stability properties. In conclusion, fibers from chestnut shells are a biodegradable and low-cost reinforcing material to improve the properties of potato starch-based films. Furthermore, it should be noted that the fibre material used as fillers in this study were not chemically treated or modified, which would lead to the development of more environmentally friendly and cheaper production process and materials.

#### CRedit authorship contribution statement

**Leonardo Amaral:** Conceptualization, Methodology, Writing – original draft, Writing – review & editing. **Francisca Rodrigues:** Supervision, Resources, Methodology, Writing – review & editing. **Aurora Silva:** Formal analysis, Data curation, Writing – review & editing. **Paulo Costa:** Supervision, Formal analysis, Data curation, Writing – review & editing. **Cristina Delerue-Matos:** Supervision, Resources, Writing – review & editing. **Elsa F. Vieira:** Conceptualization, Supervision, Investigation, Methodology, Writing – original draft, Writing – review & editing.

#### Declaration of Competing Interest

The authors declare that they have no known competing financial interests or personal relationships that could have appeared to influence the work reported in this paper.



## Data availability

No data was used for the research described in the article.

## Acknowledgments

The authors are grateful to Sortegel for the chestnut samples. This work received financial support from project “PTDC/ASP-AGR/29277/2017 - *Castanea sativa* shells as a new source of active ingredients for functional food and cosmetic applications: a sustainable approach”, supported by national funds by FCT/MCTES and co-supported by Fundo Europeu de Desenvolvimento Regional (FEDER) throughout COMPETE 2020 – Programa Operacional Competitividade e Internacionalização (POCI-01-0145-FEDER-029277). This work was also financial supported by the project Chestfilm, supported by “La Caixa” Foundation and Fundação para a Ciência e Tecnologia through the 4<sup>th</sup> edition of Promove program “O Futuro do Interior”, and by UID/QUI/50006/2020, with funding from FCT/MCTES through national funds and by the Research Unit on Applied Molecular Biosciences - UCIBIO, which is financed by national funds from FCT/MCTES (UIDP/04378/2020 and UIDB/04378/2020) and the project LA/P/0140/2020 of the Associate Laboratory Institute for Health and Bioeconomy - i4HB. Francisca Rodrigues and Elsa F. Vieira acknowledge the FCT for their work contracts (CEECIND/01886/2020 and CEECIND/03988/2018, respectively), supported by national funds (OE). Authors also thanks the project SYSTEMIC “an integrated approach to the challenge of sustainable food systems: adaptive and mitigatory strategies to address climate change and malnutrition“. The Knowledge hub on Nutrition and Food Security, has received funding from national research funding parties in Belgium (FWO), France (INRA), Germany (BLE), Italy (MIPAAF), Latvia (IZM), Norway (RCN), Portugal (FCT), and Spain (AEI) in a joint action of JPI HDHL, JPI-OCEANS and FACCE-JPI launched in 2019 under the ERA-NET ERA- HDHL (no 696295).

## Appendix A. Supplementary data

Supplementary data to this article can be found online at <https://doi.org/10.1016/j.foodchem.2022.133609>.

## References

- Ali, A., Ali, S., Yu, L., Liu, H., Khalid, S., Hussain, A., ... Ying, C. (2019). Preparation and characterization of starch-based composite films reinforced by apricot and walnut shells. *Journal of Applied Polymer Science*, 136(38), 47978. <https://doi.org/10.1002/app.47978>
- Bangar, S. P., Purewal, S. S., Trif, M., Maqsood, S., Kumar, M., Manjunatha, V., & Rusu, A. V. (2021). Functionality and applicability of starch-based films: An eco-friendly approach. *Foods*, 10(9), 2181. <https://doi.org/10.3390/foods10092181>
- Cheng, G., Zhou, M., Wei, Y. J., Cheng, F., & Zhu, P. X. (2019). Comparison of mechanical reinforcement effects of cellulose nanocrystal, cellulose nanofiber, and microfibrillated cellulose in starch composites. *Polymer Composites*, 40(S1), E365–E372. <https://doi.org/10.1002/pc.24685>
- Collazo-Bigliardi, S., Ortega-Toro, R., & Chiralt Boix, A. (2018). Reinforcement of thermoplastic starch films with cellulose fibres obtained from rice and coffee husks. *Journal of Renewable Materials*, 6(6), 599–610. <https://doi.org/10.32604/JRM.2018.00127>
- Dias, A. B., Müller, C. M., Larotonda, F. D., & Laurindo, J. B. (2011). Mechanical and barrier properties of composite films based on rice flour and cellulose fibers. *LWT-Food Science and Technology*, 44(2), 535–542. <https://doi.org/10.1016/j.lwt.2010.07.006>
- Domene-López, D., Delgado-Marín, J. J., Martín-Gullón, I., García-Quesada, J. C., & Montalbán, M. G. (2019). Comparative study on properties of starch films obtained from potato, corn and wheat using 1-ethyl-3-methylimidazolium acetate as plasticizer. *International Journal of Biological Macromolecules*, 135, 845–854. <https://doi.org/10.1016/j.ijbiomac.2019.06.004>
- Dos Santos, B. H., de Souza do Prado, K., Jacinto, A. A., & da Silva Spinacé, M. A. (2018). Influence of sugarcane bagasse fiber size on biodegradable composites of thermoplastic starch. *Journal of Renewable Materials*, 6(2), 176–182. <https://doi.org/10.7569/JRM.2018.634101>
- European Commission (2018). A European strategy for plastics in a circular economy. Communication from the Commission to the European Parliament, the Council, the European Economic and Social Committee and the Committee of the Regions. Brussels, January 16<sup>th</sup> 2018. Available online: <https://ec.europa.eu/environment/circular-economy/pdf/plastics-strategy.pdf>. [Accessed 28th Jan 2022].
- FAO. (2019). Available from: [http://www.fao.org/faostat/en/?#clcid=IwAROHODyYs-D3AYvKvJfj3cUdldYfkQjpT3tjN5IE9KukB38Im\\_TUUXZMY#data/QC/visualize](http://www.fao.org/faostat/en/?#clcid=IwAROHODyYs-D3AYvKvJfj3cUdldYfkQjpT3tjN5IE9KukB38Im_TUUXZMY#data/QC/visualize).
- García, N. L., Famá, L., Dufresne, A., Aranguren, M., & Goyanes, S. (2009). A comparison between the physico-chemical properties of tuber and cereal starches. *Food Research International*, 42(8), 976–982. <https://doi.org/10.1016/j.foodres.2009.05.004>
- Gonçalves, I., Lopes, J., Barra, A., Hernández, D., Nunes, C., Kapusniak, K., Kapusniak, J., Evtuygin, D. V., Lopes da Silva, J. A., Ferreira, P., & Coimbra, M. A. (2020). Tailoring the surface properties and flexibility of starch-based films using oil and waxes recovered from potato chips byproducts. *International Journal of Biological Macromolecules*, 163, 251–259. <https://doi.org/10.1016/j.ijbiomac.2020.06.231>
- Grossman, A., & Vermerris, W. (2019). Lignin-based polymers and nanomaterials. *Current Opinion in Biotechnology*, 56, 112–120. <https://doi.org/10.1016/j.copbio.2018.10.009>
- Hamed, I., Jakobsen, A. N., & Lerfall, J. (2021). Sustainable edible packaging systems based on active compounds from food processing byproducts: A review. *Comprehensive Reviews in Food Science and Food Safety*, 21(1), 198–226. <https://doi.org/10.1111/1541-4337.12870>
- Harini, K., Mohan, C. C., Ramya, K., Karthikeyan, S., & Sukumar, M. (2018). Effect of *Punica granatum* peel extracts on antimicrobial properties in walnut shell cellulose reinforced bio-thermoplastic starch films from cashew nut shells. *Carbohydrate Polymers*, 184, 231–242. <https://doi.org/10.1016/j.carbpol.2017.12.072>
- Lisitsyn, A., Semenova, A., Nasonova, V., Polishchuk, E., Revutskaya, N., Kozyrev, I., & Kotenkova, E. (2021). Approaches in animal proteins and natural polysaccharides application for food packaging: Edible film production and quality estimation. *Polymers*, 13(10), 1592. <https://doi.org/10.3390/polym13101592>
- Lomeli-Ramírez, M. G., Kestur, S. G., Manríquez-González, R., Iwakiri, S., De Muniz, G. B., & Flores-Sahagun, T. S. (2014). Bio-composites of cassava starch-green coconut fiber: Part II—Structure and properties. *Carbohydrate Polymers*, 102, 576–583. <https://doi.org/10.1016/j.carbpol.2013.11.020>
- Mariana, M., Alfatih, T., Yahya, E. B., Olaiya, N. G., Nuryawan, A., Mistar, E. M., Abdullah, C. K., Abdulmadjid, S. N., & Ismail, H. (2021). A current advancement on the role of lignin as sustainable reinforcement material in biopolymeric blends. *Journal of Materials Research and Technology*, 15, 2287–2316. <https://doi.org/10.1016/j.jmrt.2021.08.139>
- Matthews, C., Moran, F., & Jaiswal, A. K. (2021). A review on European Union’s strategy for plastics in a circular economy and its impact on food safety. *Journal of Cleaner Production*, 283, Article 125263. <https://doi.org/10.1016/j.jclepro.2020.125263>
- Menzel, C. (2020). Improvement of starch films for food packaging through a three-principle approach: Antioxidants, cross-linking and reinforcement. *Carbohydrate Polymers*, 250, Article 116828. <https://doi.org/10.1016/j.carbpol.2020.116828>
- Morana, A., Squillaci, G., Paixão, S. M., Alves, L., Cara, F. L., & Moura, P. (2017). Development of an energy biorefinery model for chestnut (*Castanea sativa* Mill.) shells. *Energies*, 10(10), 1504. <https://doi.org/10.3390/en10101504>
- Piñeros-Hernandez, D., Medina-Jaramillo, C., López-Córdoba, A., & Goyanes, S. (2017). Edible cassava starch films carrying rosemary antioxidant extracts for potential use as active food packaging. *Food Hydrocolloids*, 63, 488–495. <https://doi.org/10.1016/j.foodhyd.2016.09.034>
- Pinto, D., Vieira, E. F., Peixoto, A. F., Freire, C., Freitas, V., Costa, P., ... Rodrigues, F. (2021). Optimizing the extraction of phenolic antioxidants from chestnut shells by subcritical water extraction using response surface methodology. *Food Chemistry*, 334, Article 127521. <https://doi.org/10.1016/j.foodchem.2020.127521>
- Prabha, P. H., & Ranganathan, T. V. (2018). Process optimization for evaluation of barrier properties of tapioca starch based biodegradable polymer film. *International Journal of Biological Macromolecules*, 120, 361–370. <https://doi.org/10.1016/j.ijbiomac.2018.08.100>
- Silva, V. D. M., Macedo, M. C. C., Rodrigues, C. G., dos Santos, A. N., e Loyola, A. C. d. F., & Fante, C. A. (2020). Biodegradable edible films of ripe banana peel and starch enriched with extract of *Eriobotrya japonica* leaves. *Food Bioscience*, 38, Article 100750. <https://doi.org/10.1016/j.fbio.2020.100750>
- Souza de Miranda, C., Ferreira, M. S., Magalhães, M. T., Gonçalves, A. P. B., Carneiro de Oliveira, J., Guimarães, D. H., & José, N. M. (2015). Effect of the glycerol and lignin extracted from Piassava fiber in cassava and corn starch films. *Materials Research*, 18, 260–264. <https://doi.org/10.1590/1516-1439.370414>
- Versino, F., & García, M. A. (2014). Cassava (*Manihot esculenta*) starch films reinforced with natural fibrous filler. *Industrial Crops and Products*, 58, 305–314. <https://doi.org/10.1016/j.indcrop.2014.04.040>
- Wu, J., Du, X., Yin, Z., Xu, S., Xu, S., & Zhang, Y. (2019). Preparation and characterization of cellulose nanofibrils from coconut coir fibers and their reinforcements in biodegradable composite films. *Carbohydrate Polymers*, 211, 49–56. <https://doi.org/10.1021/ie9011672>